

NISTIR 7179

*Physics-Based Modeling for WUI  
Fire Spread – Simplified Model  
Algorithm for Ignition of  
Structures by Burning Vegetation*

David D. Evans  
Ronald G. Rehm  
Elisa S. Baker



Supported in part by funds provided by  
Pacific Southwest Research Station  
Forest Service  
U.S. Department of Agriculture

**NIST**

**National Institute of Standards and Technology**  
Technology Administration, U.S. Department of Commerce



**NISTIR 7179**

***Physics-Based Modeling for WUI  
Fire Spread – Simplified Model  
Algorithm for Ignition of  
Structures by Burning Vegetation***

David D. Evans  
Ronald G. Rehm  
Elisa S. Baker

*Fire Research Division  
Building and Fire Research Laboratory  
National Institute of Standards and Technology  
Gaithersburg, MD 20899*

October 2004



**U.S. Department of Agriculture**  
Ann M. Veneman, Secretary  
**Forest Service**  
Dale N. Bosworth, Chief  
**Pacific Southwest Research Station**  
James Sedell, *Director*

**U.S. Department of Commerce**  
Donald L. Evans, *Secretary*  
**Technology Administration**  
Phillip J. Bond, *Under Secretary for Technology*  
**National Institute of Standards and Technology**  
Arden L. Bement, Jr., *Director*



# TABLE OF CONTENTS

<b>LIST OF FIGURES.....</b>	<b>IV</b>
<b>LIST OF TABLES.....</b>	<b>IV</b>
<b>1.0 ABSTRACT .....</b>	<b>1</b>
<b>2.0 INTRODUCTION .....</b>	<b>1</b>
<b>3.0 BACKGROUND.....</b>	<b>2</b>
<b>3.1 PREVIOUS MODELING OF WILDLAND FUELS AND FIRES .....</b>	<b>3</b>
<b>3.2 PREVIOUS MODELING OF WUI FIRES.....</b>	<b>4</b>
<b>3.3 NIST RESEARCH CONTRIBUTION .....</b>	<b>4</b>
<b>4.0 BURNING CHARACTERISTICS OF DOUGLAS-FIR TREES .....</b>	<b>5</b>
<b>4.1 Experiments.....</b>	<b>5</b>
4.1.1 <i>Tree Preparation.....</i>	<i>5</i>
4.1.2 <i>Large Fire Laboratory.....</i>	<i>7</i>
4.1.3 <i>Instrumentation.....</i>	<i>7</i>
<b>4.2 MEASUREMENTS .....</b>	<b>8</b>
4.2.1 <i>Flame Heights.....</i>	<i>11</i>
4.2.2 <i>Heat Release Rate and Mass Loss .....</i>	<i>12</i>
4.2.3 <i>Other Measurements .....</i>	<i>13</i>
<b>4.3 ANALYSIS .....</b>	<b>13</b>
4.3.1 <i>Flame Height .....</i>	<i>13</i>
4.3.2 <i>Heat Release Rate .....</i>	<i>14</i>
<b>5.0 IGNITION OF STRUCTURES ALGORITHM FOR ECOSMART.....</b>	<b>16</b>
<b>5.1 SIMPLE ALGORITHM FOR STRUCTURE IGNITION BY BURNING LANDSCAPE TREES .....</b>	<b>17</b>
5.1.1 <i>Burnable Mass of the Tree.....</i>	<i>18</i>
5.1.2 <i>Flame Height .....</i>	<i>18</i>
5.1.3 <i>Peak Heat Release Rate .....</i>	<i>18</i>
5.1.4 <i>Radiative Fraction .....</i>	<i>19</i>
5.1.5 <i>Radiative Heat Flux.....</i>	<i>19</i>
5.1.6 <i>Ignition Criteria.....</i>	<i>19</i>
<b>6.0 IMPLEMENTATION OF THE ALGORITHM IN ECOSMART .....</b>	<b>19</b>
<b>7.0 MODELING COMPLEX PHENOMENA.....</b>	<b>20</b>
<b>8.0 RESEARCH NEEDS TO ADVANCE THE DEVELOPMENT OF PHYSICS-BASED MODELS FOR WUI AND RESIDENTIAL HOUSING COMMUNITY FIRES.....</b>	<b>22</b>
<b>9.0 NIST FIRE DYNAMIC SIMULATOR AND SMOKEVIEW MODELS .....</b>	<b>22</b>
<b>10.0 ACKNOWLEDGEMENTS .....</b>	<b>23</b>
<b>11.0 REFERENCES .....</b>	<b>24</b>
<b>APPENDIX</b>	
<b>A.....</b>	<b>29</b>
BOOKMARK NOT DEFINED.	

## LIST OF FIGURES

Figure 1 Crown height .....	6
9Figure 2a. Pictures every 5 s of the Douglas-Fir-Tree Burns starting from the application of the igniter until 55 s after that.....	9
Figure 2b. Pictures of the Douglas-Fir-Tree Burns for times between 60 s and 110 s after application of the igniter.....	10
10Figure 3 Flame height .....	11
Figure 4 HRR as a function of time .....	12
Figure 5 Flame height data.....	1313
Figure 6 Heat release rate curves aligned at their peak values .....	14
Figure 7 Triangle approximation for the heat release rate of Douglas-fir crown fires .....	15
Figure 8 – Peak heat release rate from Douglas-fir trees as a function of moisture and mass.....	16
Figure 9 Three caricatures of a house representing different levels of complexity for mathematical models .....	21

## LIST OF TABLES

Table 1 Douglas-fir tree identifications and physical measurements .....	7
Table 2 Flame heights.....	1111
Table 3 Measured peak heat release rate and burned weight loss for tree.....	12
Table 4 Tree height and flame height data.....	14

# **Physics-Based Modeling for WUI Fire Spread – Simplified Model Algorithm for Ignition of Structures by Burning Vegetation**

David D. Evans, Ronald G. Rehm, and Elisa S. Baker  
Building and Fire Research Laboratory  
National Institute of Standards and Technology

## **1.0 ABSTRACT**

A simple physics-based mathematical algorithm is described for estimating the separation distances necessary to prevent radiative ignition of structures by burning vegetation. The algorithm is directed at use in applications such as the USDA Forest Service EcoSmart software suite of tools. The algorithm represents a first step in quantifying the fire spread phenomena involving both structures and vegetation typical of wildland-urban interface (WUI) areas and residential housing communities. Results of initial experiments to characterize the heat release rate (HRR), flame height, and duration of burning for individual Douglas-fir trees are provided. In addition, research required to understand better and quantify wildland-urban and residential community fires are discussed.

## **2.0 INTRODUCTION**

The Center for Urban Forest Research, the Pacific Southwest Research Center of the U.S. Department of Agriculture (USDA) Forest Service, together with other partners, is developing a web-based suite of software tools, called EcoSmart. EcoSmart is being developed for use by individual homeowners to provide guidance in assessing the contributions of landscape vegetation to home energy conservation, land hydrology, and fire spread. EcoSmart provides means to quantify the advantages and disadvantages of landscape vegetation relative to the costs.

As a partner in this effort, with partial support from the Pacific Southwest Research Station, the Fire Research Division of the Building and Fire Research Laboratory of the National Institute of Standards and Technology (NIST) developed a simple physics-based mathematical model for estimating whether a structure will be ignited by nearby tree crown fires. This model quantifies the burning of vegetation in a manner that has not been done before. The model developed treats each tree, shrub, and house as an individual fuel element. In order to predict fire spread from burning fuel elements by ignition of other fuel elements, the ignition and burning characteristics of each fuel element and the interactions between elements has to be defined or determined. This creates a need for ignition and burning data that has not been generally measured before for vegetation and structures. With this data and appropriate models, the importance of individual fuel elements in fire propagation can be assessed. Resolving individual fuel elements in a model is necessary in order to properly evaluate the WUI and residential

housing community fires. In these areas, structures are an important asset to be protected from fire, but can be an important source of fire spread if ignited. Fire spread in the WUI or residential housing communities cannot be characterized using the methods based on fuel bed classifications that are used widely to analyze the movement of fire fronts in forest fires. Regarding each structure as a fuel element, its likely fate in a fire can only be determined by examining its possible interactions with surrounding fuel elements that can, if burning, threaten the structure. The algorithm developed in this study is the first step in creating the foundation for a new method to analyze fire threat in WUI areas and residential communities.

Version 1.0 of the fire algorithm developed by NIST is available for and compatible with the level of detail in other portions of the EcoSmart software under development. The algorithm documented in this report represents a first step in quantifying fire spread phenomena involving both structures and vegetation typical of wildland-urban areas and residential community properties. The report provides new data on HRR, flame height, and duration of burning for individual Douglas-fir trees. In addition, it also contains a discussion of research necessary to better understand and quantify wildland-urban and residential community fire spread.

### **3.0 BACKGROUND**

The development of the EcoSmart suite of software tools began at the U.S. Department of Agriculture Forest Service, Pacific Southwest Research Station in 2002. There was a need to develop an algorithm that accounted for the increased risk for home destruction by fire due to the placement of trees and other ignitable vegetation close to the structure. This factor was in opposition to the benefits these plantings may have for energy conservation and soil hydrology. Development of the EcoSmart software suite of tools was undertaken to allow property owners to evaluate advantages and disadvantages, including fire safety and economics, of planting landscaping vegetation around homes.

NIST was asked by the Pacific Southwest Research Station to develop a physics-based algorithm for ignition of structures by landscape vegetation that could be programmed into the EcoSmart suite of software tools and would be consistent with level of information and desired speed of operation of all the other parts of EcoSmart. Very little information was found in the literature that could be used to construct a physics-based model for ignition of structures by burning vegetation of the type and arrangement that would be present on landscaped properties. Principally, there was a lack of data on burning characteristics for individual trees and shrubs.

Fire is an extremely complex natural phenomenon [1-10]. Decades of research to understand and quantify fire, together with revolutionary advances in computer technology and computational algorithms, have led to the development of sophisticated mathematical models that can predict and visualize growth and spread of fire under a variety of conditions [11-16]. However, these models generally require substantial computational and data resources. Furthermore, since they have not been oriented toward



the prediction of WUI or residential community fires, they will not soon be available for application by end users without a substantial research investment over the next few years.

### **3.1 PREVIOUS MODELING OF WILDLAND FUELS AND FIRES**

Fires in the western U.S. have been headlines in the news for several recent years. Changes in the management of forested lands, the increasing intrusion of man into more remote areas and the cyclic dry periods produced by El Nino - La Nina have all increased the loss of man-made structures to fires. Wildland fires now often spread into the built environment causing injury, death and property damage. Concern about wildland fires and their effects on man and the built environment has generated increased interest recently, e.g., Livingston [17], Keller [18], Platt [19]. While the need to address fire spread in a mixed environment, containing both structures and wildland fuels, has been acknowledged, most research has continued to focus on wildland fires. Operational models that predict fire spread in wildland fuels are well developed and widely used, but do not yet address WUI fires.

For over thirty years, modeling of fire dynamics in wildland fuels has been an ongoing research and development activity [20-26]. It has led to practical or “operational” models that are regularly used by land managers to predict fire growth and spread for both planned or “controlled” burns and unexpected wildland fires. These operational models have served land managers and firefighters well both for planning controlled burns and suppression of wildfires. In the United States, the mathematical models BEHAVE [11] and FARSITE [12] are two of the most widely used operational models.

Both are based upon the pioneering research of Rothermel [20, 21], who developed the framework for these models and determined many of the empirical relations used by it. In these models, wildland fuels are characterized by 13 standard fire behavior fuel types. These fuel characterizations and their behavior in wildland fires is the subject of several of the books cited above: Chandler et al [1], Chandler et al [2], Luke and McArthur [3], Pyne et al [4], and Brown and Davis [5] lists the 13 types and their characteristics.

The basic model regards all of the fuel to cover the land surface as though it were “painted” on; i.e., all of the combustible material resides in fuel beds that have no vertical extent, but are strictly two dimensional. Fire then spreads over these fuel beds as a contour which divides unburned fuel from burned fuel or combustion products. Fuel beds can be homogeneous or inhomogeneous, isotropic or anisotropic, and they can be composed of a single fuel type or a combination of fuel types. Furthermore, the land surface may be flat or may have significant topographical features, and all of these variations make for differences in how the fire line progresses.

Inclusion of improved descriptions of the physics in these models has progressed slowly in recent years and has not taken advantage of the revolution in computer hardware, and computational algorithms and software that has occurred over this same time frame.

By comparison, over the past few decades, many of the physical and chemical processes occurring in fires have become much better understood, and physics-based mathematical and computational models have been developed to take advantage of this improved understanding. One such example is the work of Clark [27] and colleagues in which the coupling between large-scale wildland fires and the atmosphere has been studied. Another is modeling of the growth and spread of fires in structures, which has advanced dramatically using the methods of computational fluid dynamics (CFD) and, more generally, mathematical and computational methods that may be described as computational mechanics and computational combustion [28-31].

For models of combustion, the usual length scales of interest are measured in very small fractions of a meter (millimeters or less) to meters. Alternately, for problems related to computational mechanics or CFD, the length scales of interest can vary between meters and tens or even hundreds of meters. These scales should be contrasted with models for wildland fires, where the lengths are measured in kilometers or even hundreds of kilometers.

### **3.2 PREVIOUS MODELING OF WUI FIRES**

Very little progress has been made on understanding and predicting fire spread at the Wildland-Urban Interface (WUI), where both wildland fuels and man-made structures coexist. At the WUI, the length scales are intermediate to the wildland scales on the one hand and to those associated with individual structures on the other. As a result, a model for a WUI fire must describe individual structures and trees in some detail, and must be able to determine fire spread between these individual fuel sources, a much more challenging task! One of the few studies to attack this very difficult problem is the work of Maranghides [32], who concluded that there was an extreme lack of relevant data.

J. D. Cohen [33, 34] advocates the concept of a Home Ignition Zone, defined as the home and its surrounding area where heat transfer by radiation and/or convection from burning vegetation can ignite it. He is developing a model called the Structure Ignition Assessment Model (SIAM) to quantify this concept, which is being recognized as relevant to homeowners and firefighters. The model estimates conditions for home ignition. Once a home ignites in the calculation, it is considered lost. SIAM does not address the contribution of the burning structure to subsequent fire spread in the area. It therefore has limited application in the WUI, especially in cases of housing developments, where homes may be located within the Home Ignition Zone of its neighbors.

### **3.3 NIST RESEARCH CONTRIBUTION**

In order to understand better the burning of landscape trees, a series of burns was performed in the NIST large fire facility to measure the burning characteristics of individual Douglas-fir trees. The measured burning characteristics of the trees were used

as a basis for the construction of the algorithm for ignition of structures by burning vegetation.

During this research, three papers were prepared that provide background and discussion of fire spread in the wildland-urban interface and in residential housing communities [35-37]. In recent WUI fire disasters, visual evidence suggests that fully involved burning houses contribute to fire spread and destruction. Examples are given to show that the long-duration and high-intensity burning of a structure can contribute to altering the fire-generated winds [36]. In addition, early implementations of the structure ignition algorithm in EcoSmart are illustrated [35].

#### **4.0 BURNING CHARACTERISTICS OF DOUGLAS-FIR TREES**

Although landscaping trees and shrubs, if ignited, can endanger near-by structures, very little quantitative information exists about ignition and burning characteristics of landscape vegetation. Generally, experiments carried out to measure the HRR of trees have been conducted to assess the hazards of Christmas tree fires [38-40]. No information has been found to quantify how the HRR, burn duration, and flame height vary with the size of a tree or tree species. Two studies were found in which the burning characteristics of shrubs were measured [41, 42].

Previously, the HRR of dry Scotch Pine trees was measured using the instrumented hood in the Large Fire Laboratory at NIST [38]. However, the study included only one size tree. The same is true for the study of Douglas-fir tree burning carried out by Babrauskas [39]. To take advantage of existing data, in this study we continued to burn cut Douglas-fir trees. Three different commercial sizes were selected for the experiments. The height of the trees was limited by the HRR capacity of the Large Fire Laboratory exhaust hood. The tree burns provided important data for the algorithm development. Further experiments are needed to fully understand the burning characteristics. Data obtained from the burns provided information for the development of the algorithm that was not available from any other source.

#### **4.1 EXPERIMENTS**

Prior to burning, the cut trees were allowed to dry for 17 days as discussed below. All tree burns were conducted during a single week in the Large Fire Laboratory. This included time needed for instrument set-up and mounting each tree for burning. During each burn, the HRR, mass loss, flame height, vertical temperature profiles and radiant heat flux emitted from the fire were measured.

##### **4.1.1 Tree Preparation**

The Douglas-fir trees were purchased from a local nursery that grows Christmas trees. Three trees each with commercial sale heights of 1.2 m, 2.4 m, and 3.7 m (4 ft, 8 ft, and 12 ft) were cut on July 6, 2003. These trees were delivered to NIST the following day and weighed. As the trees are a large fuel load, for fire safety considerations, the trees

were dried on racks outside the Large Fire Laboratory. The racks were covered by tarps to shield the trees from rain. After 10 days, the trees were brought inside and weighed again to monitor the moisture lost to evaporation. Some of the trees had the base of the trunks trimmed to create a flat base for mounting on a stand that supported the tree upright for burning.

The trees were photographed and heights were measured (see Table 1). The crown height is the height from the bole (height of the first live branches) to the top branch as shown in Figure 1. This differs from the commercial height of the tree which is measured from the base to the tip of the stem. The crown height best represents the burnable fuel height by eliminating the top of the stem and base of the tree up to the bole height. The stem needle growth on the test Douglas-fir trees that was eliminated from the burnable mass by this definition extend 0.3 m above the highest branch in some cases, but only added a small amount to the burnable fuel mass.



Figure 1 Crown height

Tree	Test No.	Crown Height (m)	Bole Height (m)	Total Height (m)	Weight 7/7/03 (kg)	Weight 7/17/03 (kg)	Weight Pre-burn (kg)	Weight Pre-burn Initial (7/7/03)
4-1	Test 1	1.37	0.08	1.45	5.16	3.014	2.85	0.55
4-2	Test 4	1.30	0.19	1.49	3.54	1.607	1.549	0.44
4-3	Test 7	1.42	0.22	1.64	8.4	4.515	4.372	0.52
8-1	Test 2	2.31	0.27	2.58	23.11	17.597	17.597	0.76
8-2	Test 5	2.62	0.43	3.05	24.4	18.103	17.637	0.72
8-3	Test 8	2.44	0.48	2.92	40.83	29.61	28.751	0.70
12-1	Test 3	3.10	0.69	3.78	38.17	30.116	29.92	0.78
12-2	Test 9	3.20	0.71	3.91	41.26	33.08	31.92	0.77
12-3	Test 6	3.33	0.50	3.82	38.34	29.345	29.14	0.76

Table 1 Douglas-fir tree identifications and physical measurements

### 4.1.2 Large Fire Laboratory

The trees were burned in the NIST Large Fire Laboratory located on the NIST site in Gaithersburg, Maryland. The facility has several instrumented hoods that employ oxygen consumption calorimetry to measure the HRR. The largest calorimeter hood, which was used for the tree burns, has a design capacity for HRRs of 10000 kW. The hood measures 9 m x 12 m and the lower edge of the hood is 4.5 m above the floor level. At its highest, in the center of the hood, the clear space above the floor is 7.9 m. The products of combustion are collected by the hood and flow through ducts for measurement and then are exhausted from the test building. After leaving the building the fire products are treated by a pollution abatement system before being discharged into the atmosphere.

### 4.1.3 Instrumentation

The experiments were video taped from three different perspectives, and still digital photographs were also taken. The tree and stand were on a platform supported by a load cell that measured the mass loss as a function of time. Additionally, a much larger platform underneath the first was supported by load cells at each of the four corners, to verify the accuracy of the first load cell, and serve as a backup.

Additional instrumentation included the following:

Seven thermocouples were mounted on a 4.3 m (14 ft) vertical thermocouple support stand placed approximately a meter from each test tree. These thermocouples were mounted on horizontal arms at 0.61 m (2 ft) intervals, so that the sensing tips would be near the centerline of the tree crown in the buoyant gas nearest to the stem. The thermocouples were 3 mm diameter stainless steel sheathed, Type K Chomel-Alumel, 0.91 m (3 ft) long. Voltage output from the thermocouple array was recorded on the Large Fire Laboratory data acquisition system.

The first three tests had 4 water-cooled total-heat-flux gauges, which were mounted on a second 4.3 m (14 ft) vertical support located 3 m (9.8 ft) from the stem of the tree. The first gauge was located 0.61 m (2 ft) above the ground level, and the remaining three

gauges were spaced vertically every 1.22 m (4 ft). Additionally, two heat flux gauges were placed aiming upward at ground level 1.5 m (4.9 ft) and 3 m (9.8 ft) from the tree stem. For the fourth through ninth tests, a seventh heat flux gauge was added, 10 m (32.8 ft) away from tree stem. This gauge was angled at 20° to view the entire flame.

## **4.2 MEASUREMENTS**

Figure 2 presents a timeline of images from the video record of all Douglas-fir tree burns except Test 9 (tree 12-2) that was lost. Each tree was ignited at the base of the crown using a propane torch with two flames for simultaneous ignition of the crown on opposite sides of the stem. Depending on the moisture content, some trees required 5 s of torch application to ignite, others required 15 s. Once ignited, each tree was consumed by rapid burning in approximately 60 s.

All trees except Tree 12-1 behaved similarly in the burn tests. Tree 12-1 (Test 3) did not get fully involved, and required a re-ignition to sustain burning. Because of this unusual burning behavior the results for Test 3 are not included in the analysis. As there were two other trees of the same nominal size remaining in the data set, eliminating Test 3 from the analysis was regarded as not significant.

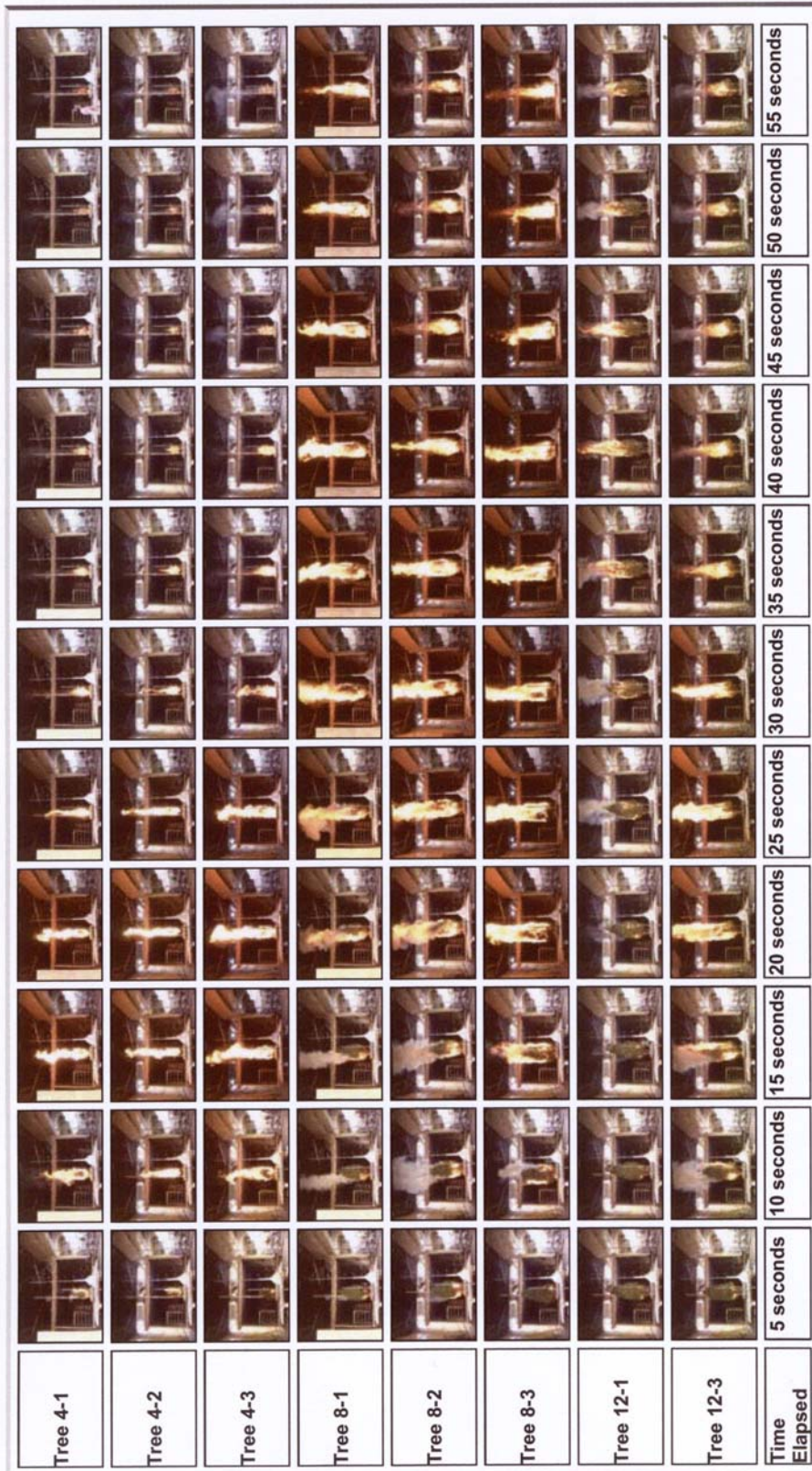


Figure 2a. Pictures every 5 s of the Douglas-Fir-Tree Burns starting from the application of the igniter until 55 s after that.



Figure 2b. Pictures of the Douglas-Fir-Tree Burns for times between 60 s and 110 s after application of the igniter.



### 4.2.1 Flame Heights

The mean flame height,  $H_{\text{flame}}$  was determined for each tree burn by analyzing video and still photos showing both the burning tree and the installed thermocouple supports. The flame height (see figure 3) was chosen to be the distance from the base of the flame near the tree bole (the lowest branch on the tree) to the top of the flame where the intermittency is 0.5. A flame intermittency of 0.5 means the visible flame is seen half of the time. For each burn, still photographs were used to determine the flame height, guided by the video record showing flame intermittency. The crown height, flame height and their ratio for each burn are shown in Table 2, and their use in the tree-burn model is presented in Sections 4.3.1 and 5.1.2.

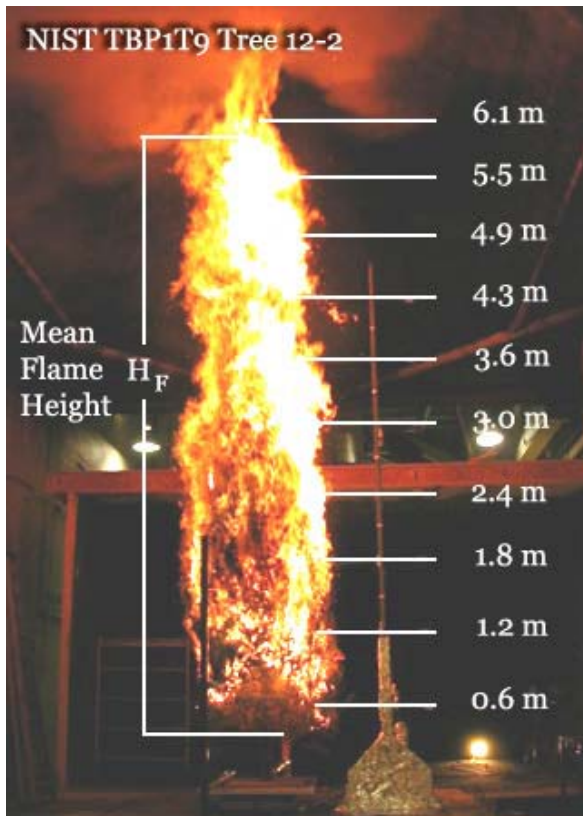


Figure 3 Flame height

Tree	$H_{\text{crown}}$ (m)	$H_{\text{flame}}$ (m)	$H_{\text{flame}}/H_{\text{crown}}$
4-1	1.37	4.2	3.06
4-2	1.30	3.47	2.68
4-3	1.42	4.36	3.07
8-1	2.31	4.61	1.99
8-2	2.62	5.05	1.93
8-3	2.44	5.61	2.30
12-1	3.10	N/A	N/A
12-2	3.20	5.08	1.59
12-3	3.33	4.69	1.41

Table 2 Flame heights

#### 4.2.2 Heat Release Rate and Mass Loss

Figure 4 shows a plot of the measured HRR for each of the tree-burns. The peak HRR occurs at different times in part because of variation in ignition times. Peak HRR and weight loss measured during the test are recorded in Table 3. The weight loss data in Table 3 are from the measurements made by the top load cell located directly under the tree.

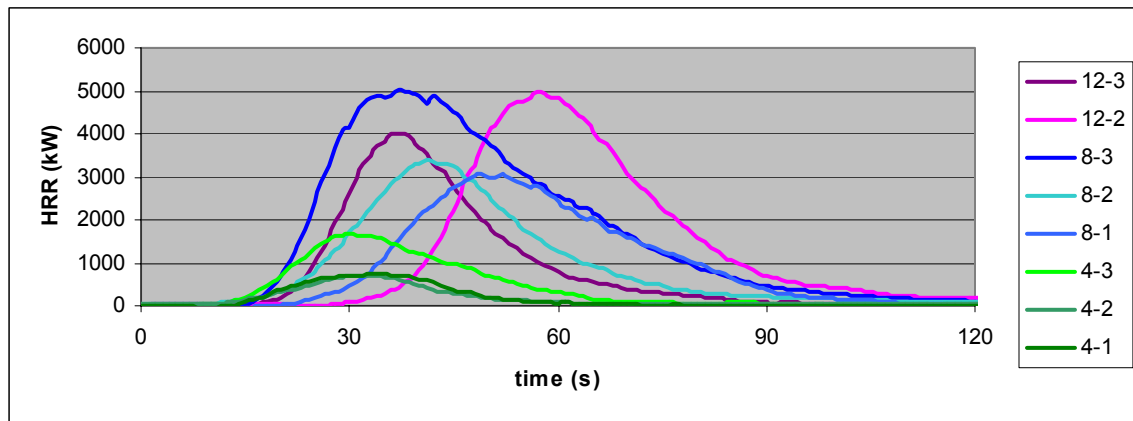


Figure 4 HRR as a function of time

Tree	HRR <sub>peak</sub> (kW)	Tree Weight Pre-burn (kg)	Weight Loss (kg)	Weight loss / pre-burn weight
4-1	780	2.85	1.44	0.51
4-2	720	1.55	1.04	0.67
4-3	1660	4.37	2.67	0.61
8-1	3350	17.60	9.13	0.51
8-2	3400	17.64	8.6	0.49
8-3	5040	28.75	12.53	0.44
12-2	5000	31.92	13.49	0.42
12-3	4000	29.14	7.91	0.27

Table 3 Measured peak HRR and burned weight loss for tree

## 4.2.2 Other Measurements

As part of the large scale experiments, many measurements, not needed immediately for the formulation of the algorithm, were recorded. These included temperature measurements from an array of thermocouples within and above the crown of the tree, and radiant and total heat flux from the fire at various distances and heights. These data will be reduced and analyzed when additional resources become available.

## 4.3 ANALYSIS

The series of tree-burn experiments provided initial data to start the formulation of the fire source portion of the algorithm to predict structural ignition from burning vegetation. Other observations from the data, not used directly in the development of the algorithm, are recorded in this section for possible use in other models for wildland-urban interface fires.

### 4.3.1 Flame Height

The mean flame heights ( $H_{\text{flame}}$ ) were compared to the crown height,  $H_{\text{crown}}$ , to determine if there was a correlation between a tree's height, and the resulting flame height. The results are shown in figure 5. Generally the larger trees produced a flame height twice the crown height. The smallest trees produced a flame three times the crown height. This data is also influenced by differences in initial moisture content. From the data in Table 1, the smallest trees lost about one-half of the initial weight before burning. The larger trees lost only one-fourth of the initial weight before burning. More experiments are needed to understand the effect of moisture and crown height on flame height. At this time, the best estimate of flame height for application to landscape trees is the data for the larger trees with greater moisture. That is  $H_{\text{flame}} / H_{\text{crown}} = 2.0$

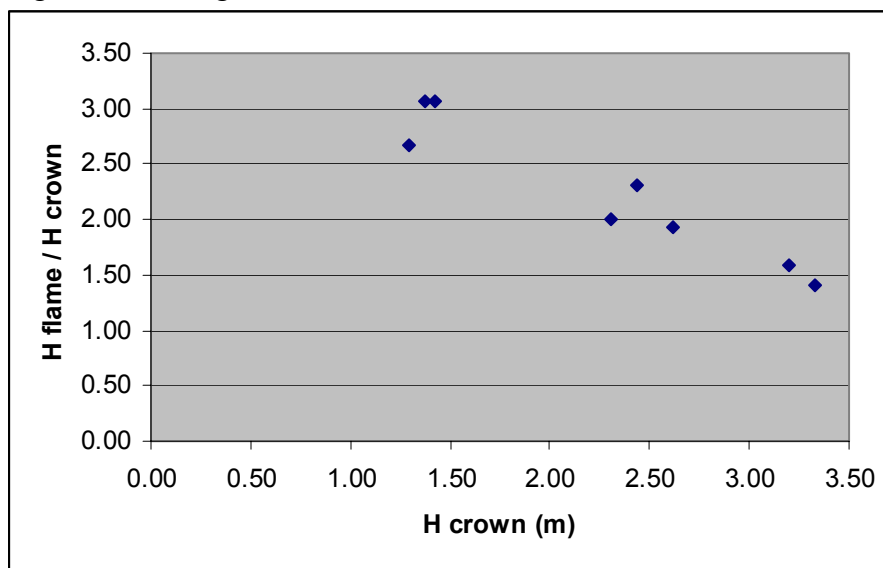


Figure 5 Flame height data

Tree	H <sub>crow</sub> n (m)	H <sub>flame</sub> (m)	H <sub>flame</sub> /H <sub>crow</sub> n
4-1	1.37	4.2	3.06
4-2	1.30	3.47	2.68
4-3	1.42	4.36	3.07
8-1	2.31	4.61	1.99
8-2	2.62	5.05	1.93
8-3	2.44	5.61	2.30
12-2	3.20	5.08	1.59
12-3	3.33	4.69	1.41

Table 4 Tree height and flame height data

### 4.3.2 Heat Release Rate

NIST tree burn experiments demonstrated that there is a similarity in the growth curves to peak HRR amongst all the trees, regardless of size. The heat release data from the experiments shows wide variation in the time to peak HRR (Figure 3). The larger trees took longer to ignite, and have a steeper rate of increase, but once the fire was steadily increasing, peak HRR was obtained in approximately 30 s for all trees. Figure 6 shows the HRR curves aligned such that the peak values occur at 30 s. From this figure, it is apparent that the size of the tree plays a large role in determining the peak HRR, but has a relatively minor affect on the length of the burn.

Using 60 s as a common time interval for burning, the HRR of the burning Douglas-fir trees can be represented well by a simple isosceles triangle shape. In this case the base of the triangle is 60 s and the height is the peak HRR. Figure 7

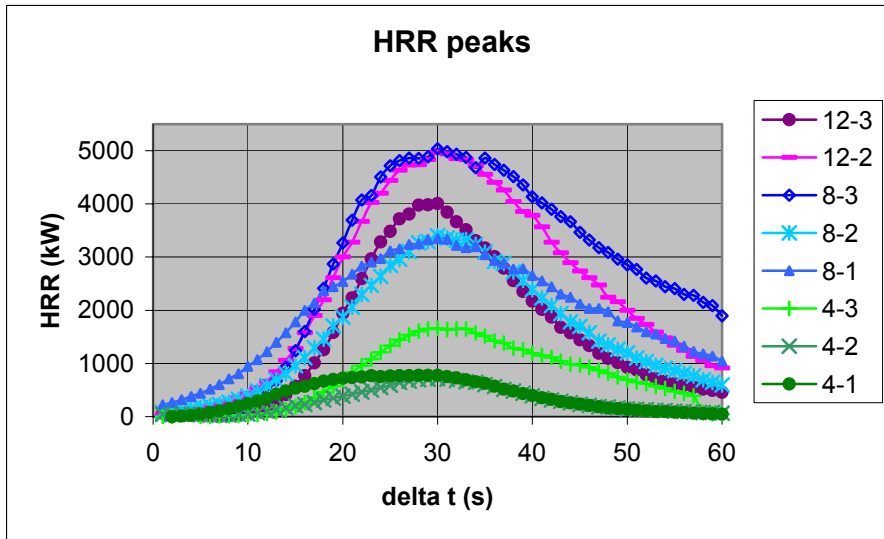


Figure 6 Heat release rate curves aligned at their peak values.

shows this approximation as it applies to two of the measured HRR curves. This result is not used in the algorithm developed in this study, but may be an important and useful approximation in future modeling of crown fires.

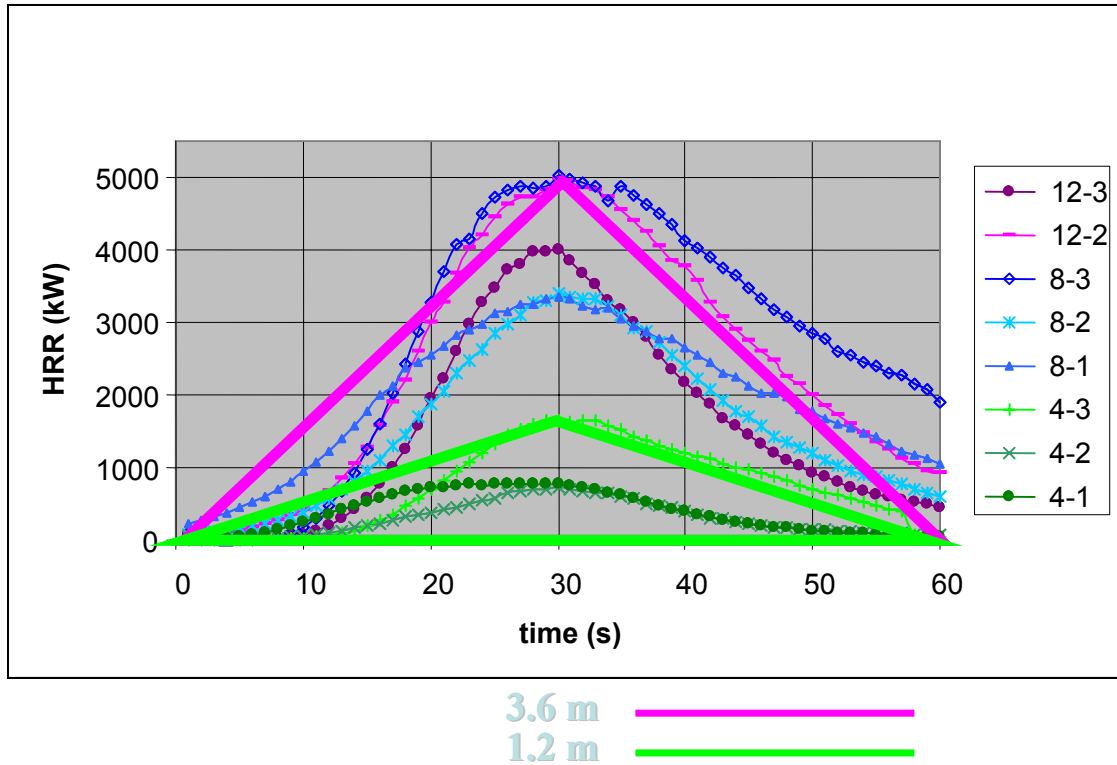


Figure 7 Triangle approximation for the heat release rate of Douglas-fir crown fires.

The burning of Douglas-fir trees has also been studied to evaluate the hazards of Christmas trees in homes. In an extensive study of Christmas-tree burns by Babrauskas [39], peak HRR were correlated with total mass of the tree and the moisture content of the needles. A plot of the correlation and the curve-fit from the published results of that study are reproduced here as Figure 8 and Equation 1.

$$q_{peak} / \text{mass} = e^{5.84 - 0.017M} \quad (1)$$

Where,

$q_{peak}$  is the peak heat release rate [kW],

mass is the total pre-burn mass of the tree [kg],

M is the moisture of the needles [mass fraction or percent by weight].

Because these results contain a quantification of the effect of moisture on the peak HRR and the trees burned were similar to those burned in this study, the results published by Babrauskas will be used in the formulation of the algorithm. As Babrauskas normalized his peak HRR using the entire mass of the cut Douglas-fir tree, his formulation will need to be modified to work with the burnable mass of the tree estimated from experiments conducted in this study.

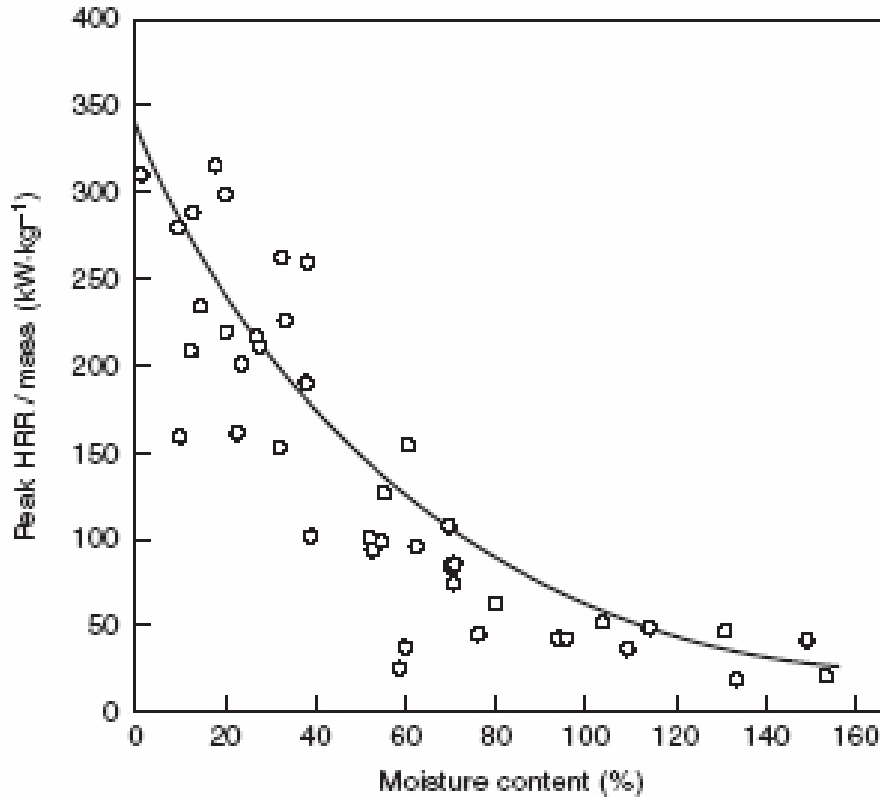


Figure 8 – Peak heat release rate from Douglas-fir trees as a function of moisture and mass [39] (reproduced with permission from the Society of Fire Protection Engineers)

## 5.0 IGNITION OF STRUCTURES ALGORITHM FOR ECOSMART

In wildland-urban and residential community areas, fire can spread rapidly, often driven by wind, to threaten homes and other structures. There are several modes by which burning vegetation can threaten a home [1-8]. For example, flames from burning trees and shrubs close to a home can ignite combustible exteriors by direct contact. In addition, small fires in collected debris, such as dry leaves and needles dropped on and around the home, can start fires at corners and in small crevices of the structure. Furthermore, ground fires, which propagate in dead debris such as leaves or pine needles or in dry live fuels such as grasses, can ignite an exterior wall. All of these mechanisms depend essentially on direct contact (convection and/or conduction) for the heating and ignition of the combustible exterior materials of the structure. Alternately, hot brands from burning trees remote from the property can be carried by the wind and blown up-against the exterior or even into homes through small openings to ignite the structure. Or, finally, for large fires, thermal radiation emitted from the flames can be transported in line-of-sight directions across open spaces to be absorbed by and ignite the structure.

Of these possible modes of fire spread, the most quantitative understanding exists for fire spread by ignition from thermal radiation [9, 10, 43-47]. For example, radiative heating

of a surface is simply additive; therefore, the radiative heat flux at a position on the surface, from two identical non-interacting burning objects oriented similarly with respect to that position, is just twice that of one of them. In addition, radiation becomes a more dominant transport mechanism as fires become larger. Crown fires, which burn intensely and spread rapidly relative to other wildland fires, are well-known examples of fires where radiation is a dominant mode for fire spread. The fact that the heat transfer by radiation from burning trees to a structure could be quantified through knowledge of the geometric relationship between the two fuel elements, lead to the selection of this mode of ignition as to be the first to be quantified in EcoSmart [48-51]. This was done with full knowledge that more often structures are ignited by other means that are not well quantified as discussed above. A simple algorithm was constructed to determine the thermal radiation transport from trees to structures.

The fire spread algorithm can be used to examine many scenarios for fire spread from vegetation to structures. The algorithm provides means to calculate the radiative heat exposure to structures from burning trees with flames located at arbitrary positions in 3-dimensions relative to structural elements.

Although it is well known that piloted radiative ignition of combustible materials depends on both the magnitude and the duration of the incident radiative heat flux [48-51], the model described here introduces only a simple critical flux assumption for ignition. To be consistent with other capabilities of the initial version of EcoSmart, the burning duration was eliminated from the algorithm for the ignition model. Fire spread from vegetation to the structure is assumed to occur, therefore, if the value of the radiative flux exceeds a critical value for ignition. In Section 5.1.6, there is additional discussion of this assumption, and a value of this critical flux.

The computational relationships that form the basis for the initial fire spread model algorithm (version 1.0) for EcoSmart are summarized below.

## **5.1 SIMPLE ALGORITHM FOR STRUCTURE IGNITION BY BURNING LANDSCAPE TREES**

The algorithm consists of six steps: 1) determine the burnable mass of the tree, 2) determine the flame height, 3) determine the peak HRR, 4) determine the fraction of the peak HRR emitted as radiative energy, 5) determine the fraction of the radiative flux emitted by the flame that impacts any part of the exterior surface, and 6) determine if the criteria for ignition of the exterior surface material is satisfied. The algorithm has been structured to utilize the burnable mass of the tree as a single parameter, to which burning properties are related. Future research may show that this single parameter can be used to generalize burning results between many different types of trees. As this study examined only one type of tree, however, experiments to determine additional data required for generalization of the results to other tree species, without generation of additional tree-burn experiments, is not recommended.

The measured mass loss during burning is used as the closest approximation to the burnable mass available for the trees burned in this study. The ratio of burnable mass for the trees to the pre-burn mass ranged from 0.27 to 0.65.

### 5.1.1 Burnable Mass of the Tree

The burnable mass of the tree is an input to the algorithm. This is often referred to as the foliar mass ( $m_{foliar}$ ) of the tree. This information is obtained from other sources within the EcoSmart software.

### 5.1.2 Flame Height

The flame height at peak burning rate is related to the crown height of the tree as shown in Figure 5. This data is complicated by the fact that both the size and the moisture content of the trees varied. More data is needed to understand the best way to relate flame height to the tree properties. For the algorithm, a fixed ratio of flame height to crown height equal to 2.0 is used. This choice is supported by the limited data. Therefore:

$$H_{flame} = 2.0 H_{crown} \quad (2)$$

where,

$H_{flame}$  [m], length of the flame above the bole of the tree,

$H_{crown}$  [m], vertical distance from the bole to the highest branch.

### 5.1.3 Peak Heat Release Rate

The peak HRR is well known to be strongly dependent on the moisture content of the burnable mass. In a study of 2 m Douglas-fir tree burning conducted by Babraukas [39] the ratio of peak HRR decreases exponentially with increasing moisture content of the needles over the range in which the tree could be ignited. The correlation developed by Babraukas relates the peak HRR of the burning tree to weight of the tree at ignition. For an algorithm to be used in EcoSmart, the data must be presented in terms of burnable mass. In the Douglas-fir trees burns conducted in this study, the pre-ignition tree weight was approximately twice the mass loss during burning (see Table 3). As this fraction of the initial tree mass lost during burning is the best approximation to the burnable mass ( $m_{foliar}$ ) available from measurement made in this study, the correlation published by Babraukas has been multiplied by the factor 2 to adjust for use with the burnable mass parameter. The peak HRR for the algorithm is:

$$\dot{q}_{peak} = 2m_{foliar} e^{5.84-0.017M} \quad (3)$$

where



$q_{peak}$  is the peak heat release rate [kW]

$m_{foliar}$  is the burnable mass of tree [kg]

M is the moisture content of the needles [in percent of the needle mass]

#### 5.1.4 Radiative Fraction

The fraction of heat emitted from a fire as thermal radiation can vary widely (see Quintiere [10]). Here, it is chosen to be a mid-range value of 0.35 (pp. 58-59 of reference [10] and HUD Report [52]).

$$q_{rad} = 0.35 q_{peak} \quad (4)$$

where,

$q_{rad}$  [kW] is the peak emitted thermal radiation from the flame

#### 5.1.5 Radiative Heat Flux

The heat flux at any part of the exterior surface of the structure is determined by a calculated view factor. The view factors are based on radiation from a vertical right cylinder body representing the flame orientated in 3-dimensions relative to the structure. The height of the cylinder is equal to the flame height ( $H_{flame}$ ), with the bottom of the cylinder position at the location of the bole of the tree. The calculation of view factors is given in Appendix A.

#### 5.1.6 Ignition Criterion

The ignition criterion for the structure is based on a critical radiant flux condition. There is no dependence on exposure time. A single value of 31.5 kW/m<sup>2</sup> is used. This value is based on criteria developed by the Department of Housing and Urban Development for safe spacing of housing from potentially large fires [52, 53]. This value is relatively high compared to minimum heat flux values needed to ignite combustible exterior materials. However, without any time dependency for the ignition model in the algorithm and using only the peak radiant energy as exposure, this value is suitable for current use.

### 6.0 IMPLEMENTATION OF THE ALGORITHM IN ECOSMART

The fire model algorithm was selected to be physics-based and to harmonize as much as practical with the other modules of EcoSmart. Many choices that were made in the development of the algorithm for ignition of structures by burning vegetation were made specifically to work within the limitations of the EcoSmart software design. There is a greater quantitative understanding of fire spread from vegetation to structures than is implemented in the software. Full and detailed models of fire development on landscaped properties have been performed with the NIST developed Fire Dynamics

Simulator (FDS) software [35-37]. Use of FDS directly in EcoSmart at this time is not practical because both the computational resources and the data requirements are too extensive. Using the algorithm developed where ignition of structures is based solely on fire radiant exposure should only be regarded as one indicator of fire spread potential from burning vegetation to structure.

As already discussed, the initial structure-ignition algorithm for EcoSmart does not account for many well known fire spread mechanisms that threaten houses. For example, the model algorithm does not contain any effect of wind. It is well known that fire spread and spread rate are enhanced by wind, see for example Chapter 5 of Quintiere [10].

Never-the-less as wind effects are not addressed in the first version of EcoSmart, they are not included in the structure-fire algorithm. Although many species of trees and shrubs will be available for use in the EcoSmart software, it was found that very little data is available that describes the burning of individual trees and shrubs in a form that is needed for the algorithm. As a result, new data was generated by NIST for burning Douglas-fir trees. As the vegetation burning portion of the algorithm was developed solely on data from Douglas-fir tree burns use of the Version 1.0 algorithm with other trees is not recommended. Additional research and data collection is needed to extend the algorithm to other tree species.

As many potentially important fire spread mechanisms have been omitted, conservative choices that favored structure ignition have been made for the fire scenarios. This is customary practice in safety analysis where considerable uncertainties exist. In the algorithm:

- All vegetation burns at the maximum burning rate.
- All surfaces ignite if exposed to a critical flux for ignition.
- Duration of burning for the sources of heat are not considered
- Duration of exposure for the materials being ignited are not considered

Since this version of EcoSmart has only implemented a model of structure ignition by thermal radiation, other important ignition threats to structures have been deferred for later development and implementation. For example, the initial version of the algorithm does not include the effects of ambient winds, burning brands and heat fluxes from nearby burning structures, for example. The determination of the relative importance of each of these effects is scenario dependent, and, therefore, inclusion of the effects will require additional research, data, and model development.

## **7.0 MODELING COMPLEX PHENOMENA**

A mathematical model of any phenomenon can be regarded as a caricature of that phenomenon. By its very nature, modeling is a creative venture. Just as a caricature depends on the artist for its rendition, so mathematical modeling depends on the modeler for its mathematical description. If a model is well crafted and efficient, it will capture

the important features of the phenomenon while ignoring less relevant ones and will produce results that are good representations of the phenomenon.

Our ability to construct effective mathematical models depends on our understanding of the phenomenon. If, for example, we do not understand a phenomenon conceptually, we will not be able to develop a mathematical representation of it. As an aside, however, any attempt to construct a mathematical model often leads to a much better understanding of research needs by focusing attention on developing relationships between variables and data some of which may not be available.

Mathematical models, even of the same phenomenon, can vary widely in complexity, as measured by several criteria: by the initial research and development effort required to construct the model, by the computational resources needed to use the model and by the data required for input and validation of the model. Using cost as the distinguishing feature, Figure 9 illustrates different classes of models by three caricatures of a house, ranging from most detailed on the left to the simplest on the right. We refer to the sketch on the left as a one-dollar model, the sketch on the right as a five cent model, and the center sketch as a 25 cent model. The price of each model is used here to convey the idea that greater model complexity generally leads to higher research and development costs, more extensive computer-resource requirements and greater data needs both for input and validation of the model. It also implies that greater model complexity usually yields a more faithful and easily understood representation of the phenomenon.

Complexity is neither a reliable gauge of model accuracy nor effectiveness. The goal of any mathematical model is to produce the simplest representation of that phenomenon consistent with user needs to understand and predict its behavior. It is generally true that representing a complex phenomenon, like fire, requires a complex model (a dollar model). For example, a simple (five cent) model, while often adequate to illustrate may be inadequate or misleading for evaluations of details.

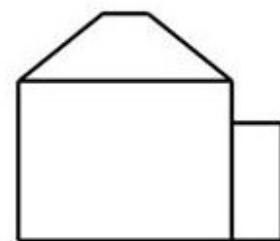


\$1

Complex Model:  
Large Computational  
and Data Needs



25¢



5¢

Approximate Model:  
Small Computational  
and Data Needs

Figure 9 Three caricatures of a house representing different levels of complexity for mathematical models.

The mathematical model algorithm for ignition of structures used in version 1.0 of Ecosmart is distinctly a 5-cent class model. As noted earlier, many choices were made throughout the development of the algorithm to simplify the model in order to approximate the ignition potential of a structure due to nearby burning vegetation, while requiring minimal computer resources and minimal input/validation data. During a review of a pre-release version of the fire portion of the EcoSmart software, many of the model limitations were identified by the reviewers. These limitations have served as the starting point for defining research needs to improve future versions of the software.

## **8.0 RESEARCH NEEDS TO ADVANCE THE DEVELOPMENT OF PHYSICS-BASED MODELS FOR WUI AND RESIDENTIAL HOUSING COMMUNITY FIRES**

As discussed above, operational models are regularly used in practice by land-managers, and fire-prediction specialists, for example, to estimate the spread and spread rate of wildland fires. However, these models are limited, as noted above, and badly need updating to take into account of current mathematical modeling methodology and the revolutionary advances in computer technology over the past few decades. Since the wildland fuels simulated in the operational models have no vertical structure, the fire growth and spread are not governed by the conservation laws of physics. Therefore, there is no hope of generalizing these models to address the problem of fire spread to buildings, transitions from ground to crown fires, or fire spread from individual tree to tree. In other words, these models will never be able to model fires at the wildland-urban interface!

When, in addition, the built environment becomes involved in a fire, as in the Oakland and Berkeley Hills fire of October 21, 1991, or more recently the Los Alamos fires in May 2000, Summerhaven, AZ, fires in June 2003, and San Diego, CA fires in October-November, 2003 these models are ineffective. The operational models cannot predict the spread of fire because the fuel load from buildings needs to be treated as discrete and three-dimensional. Also, in many cases the fuel load from structures is much larger than the surrounding vegetation. In order to model WUI and housing community fires, buildings, as well as large individual trees, must be regarded as discrete fuel elements on the length scales of interest. At a fundamental level, the empirical correlations upon which the wildland-fire operational models have been developed are no longer valid. Predictive methods are needed to address the potential fate of housing communities and individual high valued structures threatened by fire. No validated predictive models of fires in an urban or urban/wildland setting exist. Research is needed to develop three-dimensional models of fire phenomena in WUI and housing communities. Measurement of three-dimensional burning characteristics of individual vegetation and man-made structure fuel elements are needed to support the model development.

## **9.0 NIST FIRE DYNAMIC SIMULATOR AND SMOKEVIEW MODELS**

Over the past 25 years, the Building and Fire Research Laboratory (BFRL) at the National Institute of Standards and Technology (NIST) has developed a physics-based mathematical and computational model, known as the Fire Dynamics Simulator (FDS), to

predict fire phenomena inside structures. Over time, this model has been used to predict outdoor buoyant plume behavior, outdoor fire spread from structure to structure, and, most recently, fire spread in both continuous and discrete wildland fuels. FDS, and a NIST-developed companion code for visualization called Smokeview have been well documented, validated using data from large-scale indoor and outdoor experiments, and are used by hundreds of fire protection engineers around the world. The model equations and their computational implementation in FDS have been carefully selected to be computationally efficient. Therefore, while FDS is both computationally and data intensive, simulations requiring on the order of a million or more computational cells generally require only a current high-end PC running overnight. Both codes and documentation can be downloaded free of cost from the URL: <http://fire.nist.gov>.

The generation of mathematical models represented by FDS is based on the methodology of Computational Fluid Dynamics (CFD), and takes advantage of the revolutionary advances in computer technology with correspondingly reduced costs that make effective fire modeling capabilities widely available. There is a parallel between the current operational models for wildland fires and the previous generation of fire models developed by NIST in the 1980's. These "zone-models" were effective in computing fire phenomena in structures, but only as average conditions on a room-by-room basis. The need for engineers to resolve greater details within rooms forced a transition to the present generation of FDS fire modeling. To advance fire modeling of WUI and residential communities, a new generation fire modeling tools must be developed for general use by land managers, community authorities, and property owners.

At this time, there seems to be little to no research activity within the wildland-fire community directed at developing the next generation of three-dimensional fire models. NIST has begun to expand the capabilities of the FDS fire model and Smokeview fire visualization software to predict important fire phenomena occurring in the WUI and residential housing communities. This is a giant modeling undertaking. To estimate the order of magnitude of the research task to develop and validate a next-generation fire model, it has been estimated that NIST and its other agency partners have invested about 100 scientific staff-years in the development of the present FDS and Smokeview tools!

## **10.0 ACKNOWLEDGEMENTS**

The authors would like to thank Ms. Lisa Mabli for her enthusiastic support of this study with her insight into burning behavior and initial data on burning properties of vegetation. Initial data analysis and model development support was provided by Ms. Amaryllys Puig-Berrios. She served as a visiting scientist at NIST under the supervision of Dr. David Weiss from the Pacific Southwest Research Station. Development of new model representations for burning trees was contributed Dr. Sims Hostikka while at NIST as a visiting scientist from VTT in Finland. It was further refined by Dr. William Mell, formerly at the University of Utah, but now at NIST. Through the assistance of Mr. Alexander Maranghides and the operating technicians in the Large Fire Laboratory the tree burning experiments were conducted easily to produce the new data critical to the development of this model. Mr. Herbert Spitzer, Jr. contributed substantially in the

review of the implementation of the algorithm in a pre-release version of EcoSmart. His comments were an initial guide to the research needs for further development of the WUI models. This research was funded in part by the Center for Urban Forest Research, Pacific Southwest Research Station, U.S. Department of Agriculture Forest Service. Dr. E. Gregory McPherson provided continued encouragement and coordination in the development of the algorithm.

## 11.0 REFERENCES

1. Chandler, Craig, Philip Cheney, Philip Thomas, Louis Trabaud and Dave Williams. 1983. *Fire in Forestry: Volume I Forest Fire Behavior and Effects*, Wiley-Interscience, John Wiley and Sons, New York.
2. Chandler, Craig, Philip Cheney, Philip Thomas, Louis Trabaud and Dave Williams. 1983. *Fire in Forestry: Volume II Forest Fire Management*, Wiley-Interscience, John Wiley and Sons, New York.
3. Luke, R. Harry and A.G. McArthur. 1978. *Bushfires in Australia*. Australian Government Publishing Service, Canberra.
4. Pyne, Stephen J., Patricia L. Andrew and Richard D. Laven, , 1996. *Introduction to Wildland Fire*, second edition, John Wiley & Sons, Inc. New York.
5. Brown, Arthur A. and Kenneth P. Davis. 1973. *Forest Fire Control and Use*, second edition, McGraw-Hill Book Company, New York.
6. Johnson, E.A. and Miyanishi, M. (editors), *Forest Fires, Behavior and Ecological Effects*, Academic Press, San Diego, California. 2001.
7. Albini, Frank A. 1984. *Wildland Fires*, *American Scientist*, 590-597.
8. Pitts, W.M. 1991. *Wind Effects on Fires*. *Prog. Energy Combust. Sci.* 17:83-134.
9. Drysdale, Dougal. 1985. *An Introduction to Fire Dynamics*, Wiley-Interscience Publications, John Wiley and Sons, New York.
10. Quintiere, James G. 1998. *Principles of Fire Behavior*. Delmar Publishers, Albany, New York.
11. Andrews, P.L., and C.D. Bevins. 1999. "BEHAVE Fire Modeling System: Redesign and Expansion. *Fire Management Notes*. 59:16-19; Web site: <http://fire.org/>.
12. Finney, M.A. and P.L. Andrews, 1999. *FARSITE - A Program for Fire Growth Simulation*. *Fire Management Notes*. 59:13-15; Web site: <http://fire.org/>.

13. McGrattan, K.B., H.R. Baum, R.G. Rehm, A. Hamins and G.P. Forney. 2000. Fire Dynamics Simulator - Technical Reference Manual. Nist Report NISTIR 6467, National Institute of Standards and Technology, Gaithersburg, Maryland.
14. McGrattan, K.B. and G.P. Forney. 2000. Fire Dynamics Simulator -- User's Manual. Nist Report NISTIR 6469, National Institute of Standards and Technology, Gaithersburg, Maryland.
15. Forney, G.P. and K.B. McGrattan. 2000. User's Guide for Smokeview Version 1.0 -- A Tool for Visualizing Fire Dynamics Simulation Data. NISTIR 6513, National Institute of Standards and Technology, Gaithersburg, Maryland..
16. Linn, R., J. Reisner, J. Colman, J. Winterkamp, 2002. Studying Wildfire Behavior using FIRETEK, *International Journal of Wildland Fire*, 11: 233-246.
17. Livingston, R., Organizer, 2000. Second USGS Fire Science Workshop. Los Alamos, New Mexico.
18. Keller, C., Organizer. 2000. Integrating Research on Wildland Fuels and Fires. Los Alamos, New Mexico.
19. Platt, R., Roundtable Chair 200. Natural Disasters Roundtable, Forum on Urban/Wildland Fire. 26 January, National Academy of Sciences. Washington, D.C.
20. Rothermel, Richard C. 1972. A Mathematical Model for Predicting Fire Spread in Wildland Fuels. USDA Forest Service Research Paper INT-115, Intermountain Forest and Range Experiment Station, Missoula Montana? Ogden Utah?.
21. Rothermel, Richard C. 1983. How to Predict the Spread and Intensity of Forest and Range Fires. U.S. Intermountain Forest and Range Experiment Station, Ogden, Utah, Report PB 83-242289.
22. Albini, Frank A. 1985. A Model for Fire Spread in Wildland Fuels by Radiation. *Combust. Sci. and Tech.* **42**:229-258; also, Albini, Frank A. 1986. "Wildland Fire Spread by Radiation - A Model Including Fuel Cooling by Natural Convection," *Combust. Sci. and Tech.* **45**:101-113.
23. Albini, Frank A. and Brian J. Stocks, "1986. Predicted and Observed Rates of Spread of Crown Fires in Immature Jack Pine," *Combust. Sci. and Tech.* **48**:65-76.
24. Albini, Frank A. 1997. "An Overview of Research on Wildland Fire." Proceedings of the Fifth International Symposium on Fire Safety Science, Yuji Hasemi, editor.
25. Albini, F.A.. 1983. "Transport of Firebrands by Line Thermals," *Comb. Sci. & Tech.***32**:277-288.

26. Albini, F.A.. 1981. Spot Fire Distance from Isolated Sources -- Extensions of a Predictive Model. Research Note INT-309, Dept. of Agriculture, Forest Service, Intermountain Forest and Range Experiment Station, Ogden Utah
27. Clark, T.L., M.A. Jenkins, J. Coen and D. Packham. 1996. A Coupled Atmospheric-Fire Model: Convective Feedback on Fire-line Dynamics. *J. Applied Meteorology* 35:875-901.
28. Baum, H.R., K.B. McGrattan and R.G. Rehm. 1994. "Simulation of Smoke Plumes from Large Oil Fires." Twenty-Fifth Symposium (International) on Combustion, The Combustion Institute **25**:1463-1469.
29. Baum, H.R. 2000. "Large Eddy Simulations of Fire - from Concept to Computations." *Fire Protection Engineering* 6:36-42.
30. Baum, H.R. 2000. "Modeling and Scaling Laws for Large Fires." Proceedings of ISSM-III, Third International Symposium on Scale Modeling, Nagoya, Japan.
31. Baum, H.R., K.B. McGrattan and R.G. Rehm. 1994. "Mathematical Modeling and Computer Simulation of Fire Phenomena." *Theoretical and Computational Fluid Dynamics* 6:125-139.
32. Maranghides, A., 1993. Wildland-Urban Interface Fire Models, MS Thesis to Worcester Polytechnic Institute, December 8, 1993, 139pp.
- 33 Cohen, J.D., 2000. Preventing Disasters, Home Ignitability in the Wildland-Urban Interface, *Journal of Forestry*, March 2000, pp15-21.
- 34 Cohen, J.D. and Butler, B.W., 1996. "Modeling Potential Structure Ignitions from Flame Radiation Exposure with Implications for Wildland/Urban Interface Fire Management," 13th Fire and Forest Meteorology Conference, Lorne Australia, pp. 81-86.
35. Evans, D.D., R.G. Rehm, E.G. McPherson, Physics-based Modelling of Wildland-Urban Intermix Fires, Proceedings, Third International Wildland Fire Conference, October 3-6, 2003, Sydney, Australia, 2003
36. Rehm, R., D. Evans, W. Mell, S. Hostikka, K. McGrattan, G. Forney, C. Boulin, and E. Baker, Neighborhood-scale Fire Spread, Fifth Symposium on Fire and Forest Meteorology, 16-20 November, 2003, Orlando, Florida, 2003.
37. Evans, D.D., Rehm, R.G., Baker, E.S., McPherson, E.G., Wallace, J.B., 2004, Physics-based Modeling of Community Fires, Proceedings 10<sup>th</sup> International Fire Science and Engineering Conference (Interflam 2004), 5-7 July, 2004, Edinburgh, Scotland, Interscience Communications Ltd, London, United Kingdom.



38. Stroup, D.W., L. DeLauter, J. Lee and G. Roadarmel. 1999. Scotch Pine Christmas Tree Fire Tests. NIST Report of Test FR 4010, National Institute of Standards and Technology, Gaithersburg, Maryland.
39. Babrauskas, V., "Heat Release Rates", The SFPE Handbook of Fire Protection Engineering (Third Edition), Section 3, Chapter 1, p 3-1, National Fire Protection Association, Quincy, Massachusetts 02269, 2002
40. Damant, G. and S. Nurbakhsh, "Christmas Trees – What Happens When They Ignite?" Fire and Materials, 18, PP 916, 1994.
41. Jennings, C.M., Development of Protocols for Testing the Exterior Components and Assemblies of Residential Structures Under Simulated Wildfire Conditions, MS Thesis in Wood Science and Technology, University of California, Forest Products Laboratory, Richmond, California, 2000.
42. Etlinger, M.G., Fire Performance of Landscape Plants, MS Thesis in Wood Science and Technology, University of California, Santa Barbara, Santa Rosa Spring 2000.
43. Hottel, H.C. and A.F. Sarofim, Radiative Transfer, 1967, McGraw-Hill Book Company, New York, New York.
44. Siegel, R. and Howell, J.R., Thermal Radiation Heat Transfer, Third Edition, Hemisphere Publishing Corporation, Washington DC, Chapters 6 and 7.
45. Howell, J.R., Website: <http://www.me.utexas.edu/~Howell/>
- 46.. Beyler, Craig L. (Task Group Chairman), Engineering Guide: Assessing Flame Radiation to External Targets from Pool Fires, The SFPE Task Group on Engineering Practices, June 1999 (FRIS R0000329) National Fire Protection Association, Quincy, Mass.
47. Krishna S. Mudan and Paul A. Croce, Geometric View Factors, Fire Hazard Calculations for Large Open Hydrocarbon Fires, Section 2/Chapter 4, SFPE Handbook of Fire Protection Engineering, 2nd Edition; National Fire Protection Association, Quincy, Mass. 1995, p 2-57 to p 2-59.
48. Cohen, J.D. and Butler, B.W., "Modeling Potential Structure Ignitions from Flame Radiation Exposure with Implications for Wildland/Urban Interface Fire Management," 13<sup>th</sup> Fire and Forest Meteorology Conference, Lorne Australia, 1996, pp. 81-86.
49. Cohen, J.D., 2000. Preventing Disasters, Home Ignitability in the Wildland-Urban Interface, *Journal of Forestry*, PP 15-21, March 2000.
50. Cohen, J.D., 2001. Wildland-urban fire--a different approach. In: Proceedings of the Firefighter Safety Summit, Nov. 6-8, 2001, Missoula, MT. Fairfax, VA: International Association of Wildland Fire. ([www.umt.edu/ccesp/wfs/proceedings/Jack D. Cohen.doc](http://www.umt.edu/ccesp/wfs/proceedings/Jack_D._Cohen.doc))

51. Cohen, J.D., "What is the Wildland Fire Threat to Homes," The Thompson Memorial Lecture, April 10, 2000, School of Forestry, Northern Arizona University, Flagstaff, Arizona.

52. Department of Housing and Urban Development. Siting of HUD-Assisted Projects near Hazardous Facilities – A Guidebook, Acceptable Separation Distances from Explosive and Flammable Hazards, September 1996, Department of Housing and Urban Development Report HUD-1060-CPD (1).

53. Department of Housing and Urban Development, *Safety Considerations in Siting Housing Projects*, 1975, Housing and Urban Development Report 0050137.

## Model Geometry

### Configuration Factor for the Cylindrical Flame of a Burning Conifer and an Element on the Target Structure.

The radiation exchange between individual elements (structures, trees, shrubs, etc.) at the Wildland-Urban Interface (WUI) can be analyzed by the configuration-factor (CF) approach presented, for example, by Hottel and Sarofim [1] or by Siegel and Howell [2], among others. Such an approach has been used by the Society of Fire Protection Engineers (SFPE) [3], [4] to assess the thermal radiation to an external target from a pool fire. According to this analysis [3], three major steps are required:

1. Estimation of the characteristics of the pool fire, such as its radius, its flame height and its burning rate.
2. Estimation of the thermal radiation characteristics of the fire; e.g., its average emissive power, and
3. Calculation of the incident radiant flux at the target location.

Calculation of the incident radiant flux at a target structure can be accomplished by using the CF approach. In this approach, the radiative exchange from an elemental area of the flame to an elemental area on the target is the fraction of the total energy per unit time leaving the elemental flame area and incident upon elemental target area. This fraction depends upon the normal angles of the emitting and the receiving surfaces and the distance between the two surfaces.

### CF between a Finite-Length, Vertical Cylinder and a Differential Element on the Exterior of a Structure.

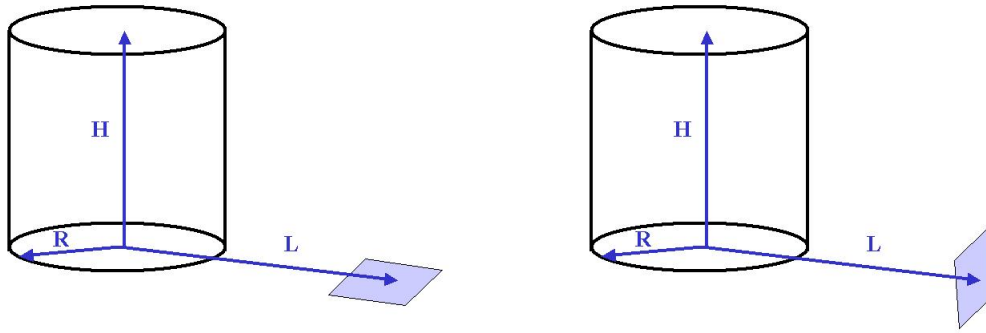


Figure 1: Schematic diagrams show the geometrical relationship between a finite-length, vertical circular cylinder, representation of a flame and a horizontal or a vertical elemental area at ground level.

Figure 1 shows a schematic diagram of a pool-fire flame modelled as a vertical, circular cylinder of height  $H$  and radius  $R$ . The radiation from this model flame impinges on a vertical rectangular element at ground level at a horizontal distance  $L$  from the axis of the cylindrical flame in the left diagram of Figure 1 and a horizontal rectangular element in the right diagram. The Configuration Factor (CF), or the view factor, determines the fraction of the radiation from the flame that is incident on each target element.  $F_{12,H}$  is the CF for a horizontal target element and  $F_{12,V}$  is the CF for a vertical element. Shokri and Beyler [3] present analytical expressions for these Configuration Factors as functions of the two parameters,  $s$ , the dimensionless horizontal distance of the target element from the centerline of the fire, and  $h$ , dimensionless cylindrical flame height:

$$s = \frac{L}{R}, \quad h = \frac{H}{R}, \quad A = \frac{h^2 + s^2 + 1}{2s}, \quad B = \frac{s^2 + 1}{2s}$$

The CF for the horizontal element is

$$F_{12,H} = \frac{B - 1/s}{\pi\sqrt{B^2 - 1}} \tan^{-1} \sqrt{\frac{(B+1)(s-1)}{(B-1)(s+1)}} - \frac{A - 1/s}{\pi\sqrt{A^2 - 1}} \tan^{-1} \sqrt{\frac{(A+1)(s-1)}{(A-1)(s+1)}}$$

and the CF for the vertical element is

$$F_{12,V} = \frac{1}{\pi s} \tan^{-1} \left( \frac{h}{\sqrt{s^2 - 1}} \right) - \frac{h}{\pi s} \tan^{-1} \sqrt{\frac{(s-1)}{(s+1)}} + \frac{Ah}{\pi s\sqrt{A^2 - 1}} \tan^{-1} \sqrt{\frac{(A+1)(s-1)}{(A-1)(s+1)}}$$

Now consider a crown fire in a single tree. As above, we will assume that flame can be modelled as a cylinder, and assume the top of the flame extends to height  $H$  above the ground, whereas the base of the flame is at the bole height, or the height of the base of the crown  $D$ . **NIST experiments show that the flame height extends from the base of the bole to twice the crown height.** Take the midpoint of the target element to be at height  $M$  above the ground and at a horizontal distance  $L$  from the centerline of the flame. The Configuration Factors are pictured schematically in Figure 2 and can be determined by the analytical expressions above of Shokri and Beyler [3] using techniques for addition of CFs [2].

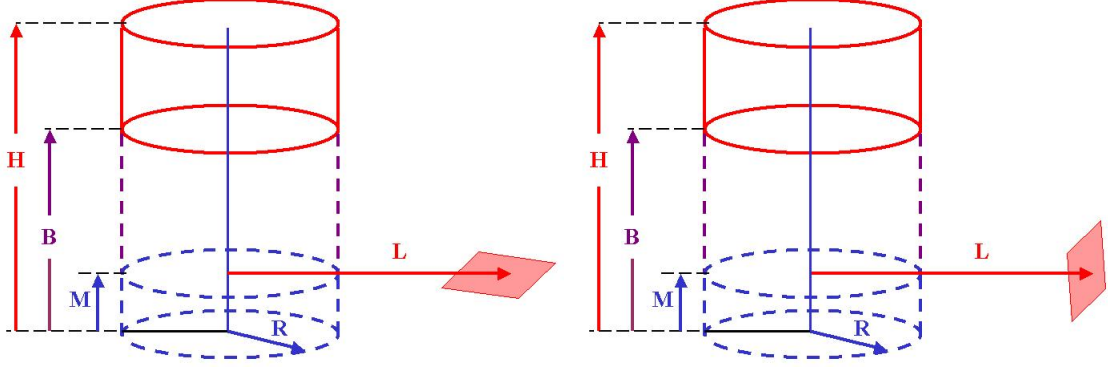


Figure 2: **Schematic diagrams showing a burning tree crown represented by a circular cylindrical flame (color red) starting at height  $D$ , the base of the crown or the top of bole, and extending to height  $H$ . NIST experiments show that the flame height extends from the base of the bole to twice the crown height. The Configuration Factor (CF) is calculated between the flame and differential vertical or horizontal elemental areas of height  $M$  above ground level and at horizontal distance  $L$  from the centerline of the flame.**

To model the CF between the crown fire and the vertical and horizontal elemental areas, we use the cylindrical-flame analysis presented above. First, take a cylinder of height  $H - M$  :

$$s = \frac{L}{R}, \quad h = \frac{(H-M)}{R}, \quad A_1 = \frac{h^2 + s^2 + 1}{2s}, \quad B = \frac{s^2 + 1}{2s}$$

For this cylinder, the CF for the horizontal element is

$$F_{12a,H} = \frac{B - 1/s}{\pi\sqrt{B^2 - 1}} \tan^{-1} \sqrt{\frac{(B+1)(s-1)}{(B-1)(s+1)}} - \frac{A_1 - 1/s}{\pi\sqrt{A_1^2 - 1}} \tan^{-1} \sqrt{\frac{(A_1+1)(s-1)}{(A_1-1)(s+1)}}$$

and for the vertical element is

$$F_{12a,V} = \frac{1}{\pi s} \tan^{-1} \left( \frac{h}{\sqrt{s^2 - 1}} \right) - \frac{h}{\pi s} \tan^{-1} \sqrt{\frac{(s-1)}{(s+1)}} + \frac{A_1 h}{\pi s \sqrt{A_1^2 - 1}} \tan^{-1} \sqrt{\frac{(A_1+1)(s-1)}{(A_1-1)(s+1)}}$$

Next, take a cylinder of height  $D - M$  :

$$s = \frac{L}{R}, \quad d = \frac{(D-M)}{R}, \quad A_2 = \frac{d^2 + s^2 + 1}{2s}, \quad B = \frac{s^2 + 1}{2s}$$

For this cylinder, the CF for the horizontal element is

$$F_{12b,H} = \frac{B - 1/s}{\pi\sqrt{B^2 - 1}} \tan^{-1} \sqrt{\frac{(B+1)(s-1)}{(B-1)(s+1)}} - \frac{A_2 - 1/s}{\pi\sqrt{A_2^2 - 1}} \tan^{-1} \sqrt{\frac{(A_2+1)(s-1)}{(A_2-1)(s+1)}}$$

and for the vertical element is

$$F_{12b,V} = \frac{1}{\pi s} \tan^{-1} \left( \frac{d}{\sqrt{s^2-1}} \right) - \frac{d}{\pi s} \tan^{-1} \sqrt{\frac{(s-1)}{(s+1)}} + \frac{A_2 d}{\pi s \sqrt{A_2^2-1}} \tan^{-1} \sqrt{\frac{(A_2+1)(s-1)}{(A_2-1)(s+1)}}$$

The two CFs describing the crown fire should then be  $F_{12,H} = F_{12a,H} - F_{12b,H}$  and  $F_{12,V} = F_{12a,V} - F_{12b,V}$ . Written out fully, then:

The CF from the crown fire to the horizontal element is

$$\begin{aligned} F_{12,H} &= \frac{B-1/s}{\pi \sqrt{B^2-1}} \tan^{-1} \sqrt{\frac{(B+1)(s-1)}{(B-1)(s+1)}} - \frac{A_1-1/s}{\pi \sqrt{A_1^2-1}} \tan^{-1} \sqrt{\frac{(A_1+1)(s-1)}{(A_1-1)(s+1)}} \\ &- \left( \frac{B-1/s}{\pi \sqrt{B^2-1}} \tan^{-1} \sqrt{\frac{(B+1)(s-1)}{(B-1)(s+1)}} - \frac{A_2-1/s}{\pi \sqrt{A_2^2-1}} \tan^{-1} \sqrt{\frac{(A_2+1)(s-1)}{(A_2-1)(s+1)}} \right) \\ &\quad \frac{A_2-1/s}{\pi \sqrt{A_2^2-1}} \tan^{-1} \sqrt{\frac{(A_2+1)(s-1)}{(A_2-1)(s+1)}} - \frac{A_1-1/s}{\pi \sqrt{A_1^2-1}} \tan^{-1} \sqrt{\frac{(A_1+1)(s-1)}{(A_1-1)(s+1)}} \end{aligned}$$

and for the vertical element is

$$\begin{aligned} F_{12a,V} &= \frac{1}{\pi s} \tan^{-1} \left( \frac{h}{\sqrt{s^2-1}} \right) - \frac{h}{\pi s} \tan^{-1} \sqrt{\frac{(s-1)}{(s+1)}} + \frac{A_1 h}{\pi s \sqrt{A_1^2-1}} \tan^{-1} \sqrt{\frac{(A_1+1)(s-1)}{(A_1-1)(s+1)}} \\ &- \left[ \frac{1}{\pi s} \tan^{-1} \left( \frac{b}{\sqrt{s^2-1}} \right) - \frac{b}{\pi s} \tan^{-1} \sqrt{\frac{(s-1)}{(s+1)}} + \frac{A_2 b}{\pi s \sqrt{A_2^2-1}} \tan^{-1} \sqrt{\frac{(A_2+1)(s-1)}{(A_2-1)(s+1)}} \right] \end{aligned}$$

where, as before,

$$\begin{aligned} s &= \frac{L}{R}, \quad h = \frac{(H-D)}{R}, \quad b = \frac{(B-D)}{R} \\ A_1 &= \frac{h^2 + s^2 + 1}{2s}, \quad A_2 = \frac{b^2 + s^2 + 1}{2s}, \quad B = \frac{s^2 + 1}{2s} \end{aligned}$$

### CF Dependence on Angles

The elemental area is regarded as part of the exterior wall of the target structure that is being irradiated by the cylindrical crown-fire flame. There is a second plane which contains the axis of the cylindrical flame and is perpendicular to the irradiated wall. This second plane contains lines perpendicular to the flame axis that determine the shortest distance between the flame and the irradiated plane or wall. Figure 3 shows a schematic diagram of the "flame," the "wall," and the other geometrical quantities discussed here.

In this geometry, the "flame" model, the "wall" and two angles define the CF. The first,  $\theta_1$ , is an elevation angle from mid-height on the cylindrical flame surface to the center of the irradiated elemental area. This angle is in the vertical plane containing the axis of the cylindrical flame, which is perpendicular to the plane of the elemental area (the second plane defined above). This angle can be written as

$$\theta_1 = \arctan \left[ \frac{(D-M) + 0.5(H-D)}{L-R} \right] = \arctan \left[ \frac{(d + 0.5(h-d))}{s-1} \right]$$

The second angle,  $\theta_2$ , is a lateral angle which is determined by the distance along the irradiated wall of the elemental area from the normal plane (plane two above). If we define by  $X$  this lateral distance, and  $x$  as  $x = X/R$ , then this second angle  $\theta_2$  can be written as

$$\theta_2 = \arctan \left[ \frac{X}{L-R} \right] = \arctan \left[ \frac{x}{s-1} \right]$$

Including the effects of the angles on the configuration factor, we have

$$CF_V = F_{12a,V} \cos \theta_1 \cos \theta_2$$

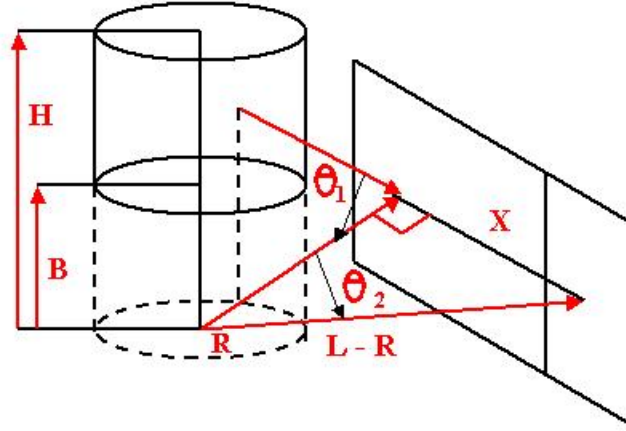


Figure 3: Schematic diagram showing the geometry for a three-dimensional configuration factor (CF) between a burning tree crown represented by a circular cylindrical flame (color red) starting at height  $D$ , the base of the crown or the top of the bole, and extending to height  $H$ . NIST experiments show that the flame height extends from the base of the bole to twice the crown height. The Configuration Factor (CF) is calculated between the flame and the middle of a differential vertical element, which is of height  $2M$ .

or,

$$CF_V / [\cos \theta_1 \cos \theta_2] = F_{12a,V}$$

Finally, substitute for  $F_{12a,V}$  :

$$CF_V = \left[ \frac{1}{\pi s} \tan^{-1} \left( \frac{h}{\sqrt{s^2 - 1}} \right) - \frac{h}{\pi s} \tan^{-1} \sqrt{\frac{(s-1)}{(s+1)}} + \frac{A_1 h}{\pi s \sqrt{A_1^2 - 1}} \tan^{-1} \sqrt{\frac{(A_1 + 1)(s-1)}{(A_1 - 1)(s+1)}} \right] \sin \theta_1 \cos \theta_2$$

$$- \left[ \frac{1}{\pi s} \tan^{-1} \left( \frac{d}{\sqrt{s^2 - 1}} \right) - \frac{d}{\pi s} \tan^{-1} \sqrt{\frac{(s-1)}{(s+1)}} + \frac{A_2 d}{\pi s \sqrt{A_2^2 - 1}} \tan^{-1} \sqrt{\frac{(A_2 + 1)(s-1)}{(A_2 - 1)(s+1)}} \right] \sin \theta_1 \cos \theta_2$$

## References

- [1] Hottel, H.C. and A.F. Sarofim, Radiative Transfer, 1967, McGraw-Hill Book Company.
- [2] Siegel, R. and Howell, J.R., *Thermal Radiation Heat Transfer*, Third Edition, Hemisphere Publishing Corporation, Washington, Chapters 6 and 7.
- [3] *Engineering Guide: Assessing Flame Radiation to External Targets from Pool Fires*, The SFPE Task Group on Engineering Practices, Craig L. Beyler, Chairman, June 1999 (FRIS R0000329).

- [4] Krishna S. Mudan and Paul A. Croce, Geometric View Factors, Fire Hazard Calculations for Large Open Hydrocarbon Fires, Section 2/Chapter 4, *SFPE Handbook of Fire Protection Engineering*, 2nd Edition; National Fire Protection Association, Quincy, Mass. 1995, p2-57 to p2-59.